Journal of International Scientific Publications:
Materials, Methods & Technologies, Volume 6, Part 1

MICROSTRUCTURE AND ELECTRICAL PROPERTIES OF MULTILAYER VARISTORS BASED ON DOPED ZINC OXIDE

Jan Kulawik, Dorota Szwagierczak, Bohdan Rusiecki, Barbara Gröger
Institute of Electron Technology, Kraków Division,
ul. Zablocie 39, 30-701 Kraków, Poland

Abstract

The paper presents fabrication procedure, microstructure and electrical properties of multilayer varistors based on ZnO doped with Bi, Sb, Co, Mn, B, Si and Pr oxides. Tape casting technique was used for preparation of flexible ceramic tapes 100 μm thick. A slurry for tape casting was prepared by ball-milling of the inorganic powder with the organic part which contains polyvinyl butyral as a binder, fish oil as a dispersant, polyethylene glycol and dibutyl phthalate as plasticizers, toluene and isopropyl alcohol as solvents. Green sheets with screen-printed Pt electrodes were stacked, pressed isostatically and cosintered at 1050°C. The microstructure and the distribution of elements inside multilayer varistors were studied using scanning electron microscopy and energy dispersive spectroscopy. Current-voltage characteristics of multilayer varistors were determined. The investigated varistors exhibit a high nonlinearity coefficient of 25-28 and a breakdown voltage of 60-80 V.

Key words: *multilayer varistor, doped ZnO, tape casting, nonlinearity coefficient*

1. INTRODUCTION

Varistor is a ceramic variable resistor which exhibits a voltage-dependent nonlinear current-voltage characteristic. Varistors are applied to protect electronic devices against voltage surges [1-3].

The current-voltage (I-V) dependence for a varistor is shown schematically in Fig.1. Three regions can be distinguished in this curve. In a region of low currents, the characteristic is almost ohmic and the resistance value is very high (about 10^9 Ω). The voltage is lower than the potential barrier at grain boundaries. In a medium current region (above the switch voltage) current I changes exponentially with voltage U ($I = CU^{\alpha}$ where: α - nonlinearity coefficient, C – constant).

In this region, the potential barrier at grain boundaries is overcome and a rapid increase in electrical conduction takes place. The value of nonlinearity coefficient $\alpha = d \log I / d \log U$ can be determined from the slope of the current-voltage characteristic. Typically, nonlinearity coefficients of oxide varistors are at a level of 20-80. For high currents, there exists a second region of linear I-U dependence related to a low intrinsic resistance of varistor grains (1-10 Ω).

Conventional varistors are produced as bulk elements based on semiconducting ceramics containing ZnO, SiC, TiO_2, $SrTiO_3$ [1-7]. The widely used varistor ceramics based on doped zinc oxide is composed of relatively large ZnO grains (about 10 μm in diameter), characterized by a relatively high electrical conductivity, surrounded by thin insulating layers built of phases rich in Bi_2O_3 and in other dopants. For fabrication of conventional bulk varistors, a typical ceramic procedure is used comprising preparation of ceramic powders followed by pressing and sintering of ceramic pellets.

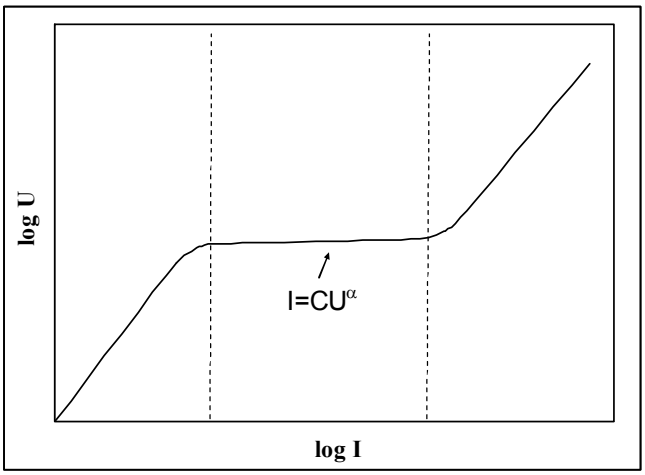


Fig. 1. Schematic plot of current-voltage characteristic of a varistor

Since the 80s of the 20th century, development of multilayer varistors (MLC) has taken place due to growing application range of low voltage circuits and strong demand for miniaturization and enhanced integration scale in electronic circuits. These varistors are fabricated by a technology analogous to that applied for multilayer capacitors – by cosintering of laminates containing several tape cast ceramic foils with screen printed internal electrodes connected in parallel [8-18]. Multilayer varistors are utilized for low voltage protection against surges caused by electrostatic discharge, atmospheric discharge, overvoltage in integrated circuits, hybrid circuits, surface mount circuits. Today, many electronic devices have their own independent supply source and work at low voltages of 3-4 V. For their surge protection, multilayer varistors are the most suitable choice.

Electrostatic barrier which is created by Bi_2O_3–rich grain boundary is about 3.5 V [2]. To some extent, the height of this barrier depends on grain boundary thickness, kind and content of dopants, sintering profile. Under applied electrical field, current flows in the part of a layer with the lowest number of grain boundaries between internal electrodes. So, to fabricate a low-voltage varistor only a small number of grain boundaries is required between electrodes. However, diminishing of the grain size distribution is essential for a good performance of multilayer varistors [8].

The paper presents the microstructure and electrical properties of multilayer varistors based on ZnO doped with Bi, Sb, Co, Mn, B, Si and Pr oxides fabricated by tape casting and cosintering of ceramic tapes with screen-printed platinum electrodes.

2. EXPERIMENTAL PROCEDURE

Tape casting technique was used for preparation of a flexible varistor ceramic tape. As shown in Table 1 the inorganic part of a slurry is based on ZnO doped with Bi_2O_3 , Si_2O_3, CoO, MnO, Cr_2O_3 , B_2O_3 , SiO_2 and Pr_2O_3. Main constituents of the inorganic part were obtained by coprecipitation method. Some dopants, such as Pr_2O_3, were introduced by mixing of the components in a ball-mill.

The organic part consists of polyvinyl butyral as a binder, fish oil as a dispersant, polyethylene glycol and dibutyl phthalate as plasticizers, toluene and isopropyl alcohol as solvents.

Flow chart for fabrication of multilayer varistors is shown schematically in Fig. 2.

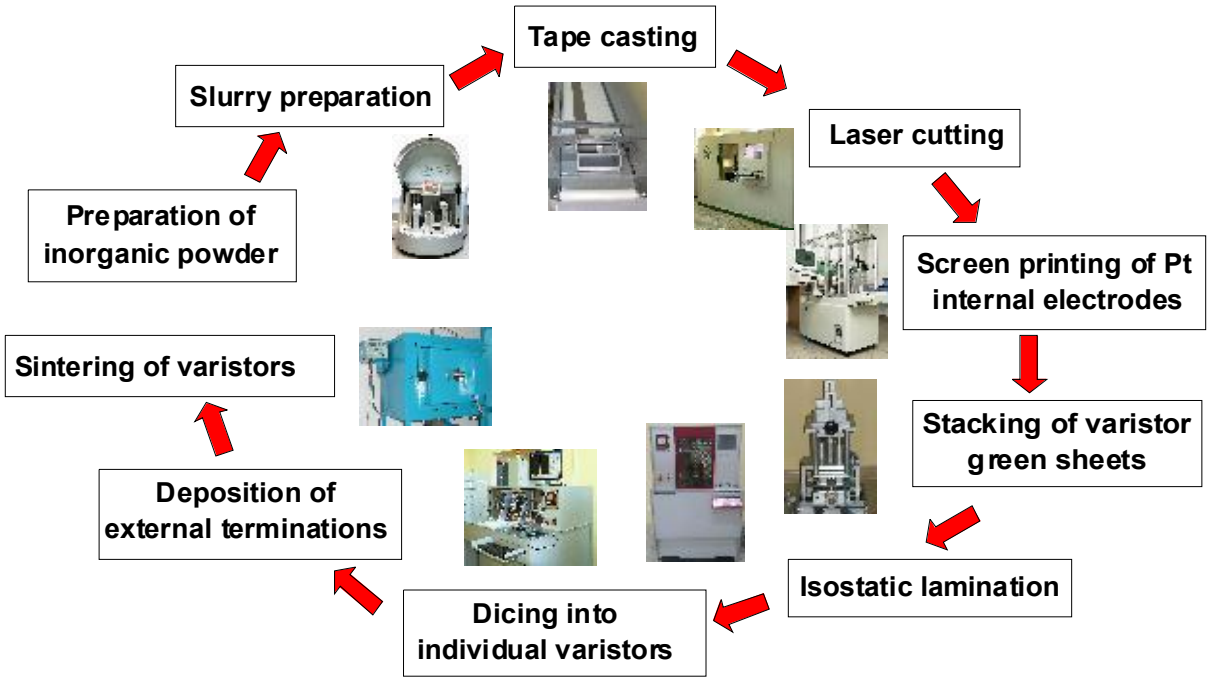


Fig. 2. Flow chart for fabrication process of multilayer varistors

Table 1. Composition of the inorganic part of the slurry for varistor tape casting

Oxide	ZnO	Bi_2O_3	Sb_2O_3	CoO	MnO	Cr_2O_3	B_2O_3	SiO_2	Pr_2O_3
Content (mol%)	96.95	0.129	0.257	0.594	0.495	0.116	0.069	0.495	0.895

The slurry was prepared by ball-milling of the inorganic powders with the organic part for 3 h. The composition of the slurry for tape casting of foils for multilayer varistors is given in Table 2.

Table 2. Composition of slurry for tape casting of varistor foil

Slurry component	Content (wt.%)
Inorganic powder	52.6
Polyvinyl butyral	7.0
Fish oil	0.9
Polyethylene glycol	2.2
Dibutyl phthalate	2.2
Isopropyl alcohol	17.5
Toluene	17.6

Tape casting was performed by a R. Mistler TTC-1200 machine. Ceramic foils were cast onto a moving polyester carrier tape covered with silicone. The green tape was dried for a few hours at room temperature and subsequently at 50°C. Then, using a laser (E-355-3-G-OA Oxford Laser) the green tape was cut into sheets with proper dimensions and holes for sheet positioning during stacking were made.

Internal electrodes from a platinum thick-film paste were screen printed on green varistor sheets. Then, five or ten layers with screen printed electrodes separated by 1-3 layers of the varistor foil were stacked and laminated isostatically (IL-4008PC Pacific Trinetics Corporation laminator) under a pressure of 35 MPa at 70°C. Subsequently, the laminates were diced into individual varistors, and external terminations of the internal electrodes connected in parallel were deposited.

The final step was firing of multilayer varistors. The temperature profile was carefully chosen to ensure slow burnout of organic components from the green tapes and from the electrode paste followed by cosintering of ceramic layers and platinum electrodes. The maximum temperature of 1050°C was maintained for 2 h to attain good densification of ceramic. The applied firing profile is shown in Fig. 3.

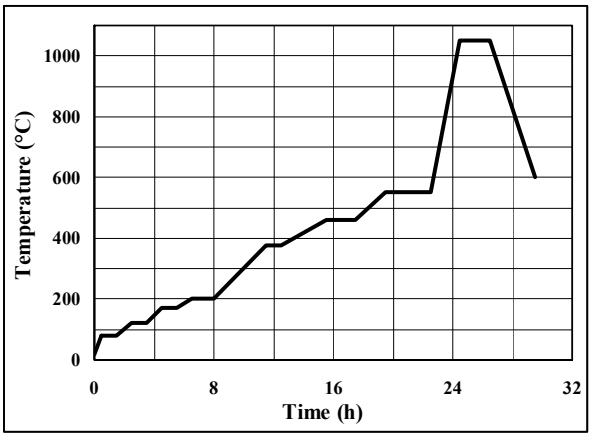


Fig. 3. Firing profile of multilayer varistors

The microstructure and distribution of elements inside multilayer varistors were studied using scanning electron microscopy (FEI Company Nova NanoSEM 200) and energy dispersive spectroscopy (EDAX EDS System, Genesis Software).

Current-voltage characteristics of multilayer varistors were determined in a voltage range of 0-110 V.

3. RESULTS AND DISCUSSION

The green varistor tape was smooth, flexibile and with a high tensile strength. Its thickness was uniform, equals to about 100 μm. In Fig. 4a a roll of the green varistor tape is shown and in Fig. 4b green sheets with screen printed Pt electrodes are presented.

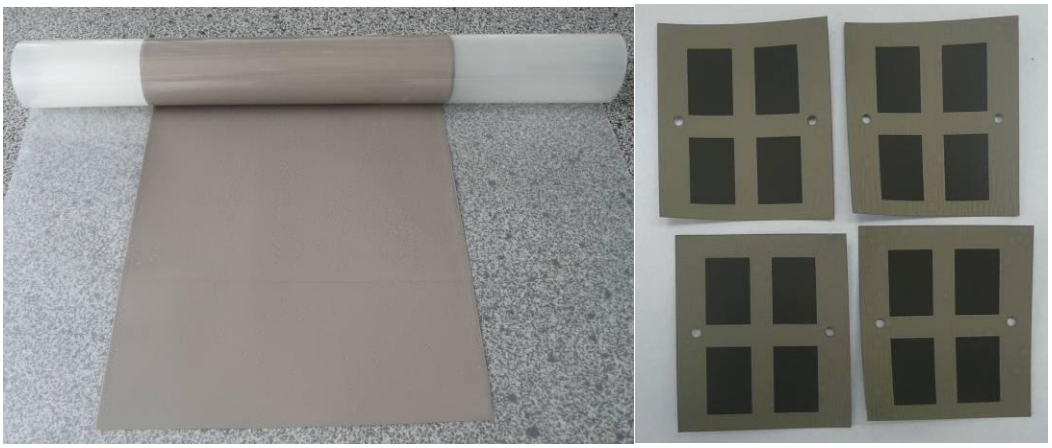
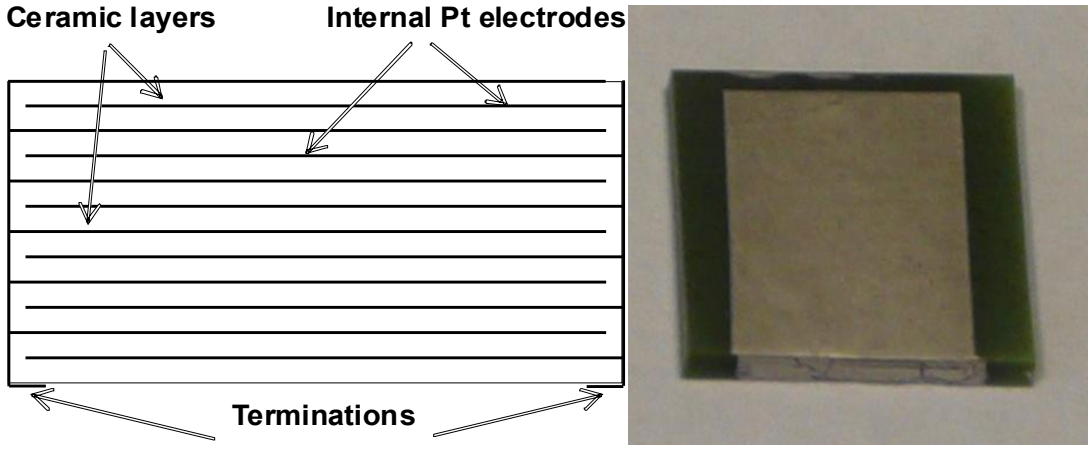


Fig. 4. (a) Flexible green varistor tape, (b) green sheets with screen printed Pt electrodes for 4 varistors

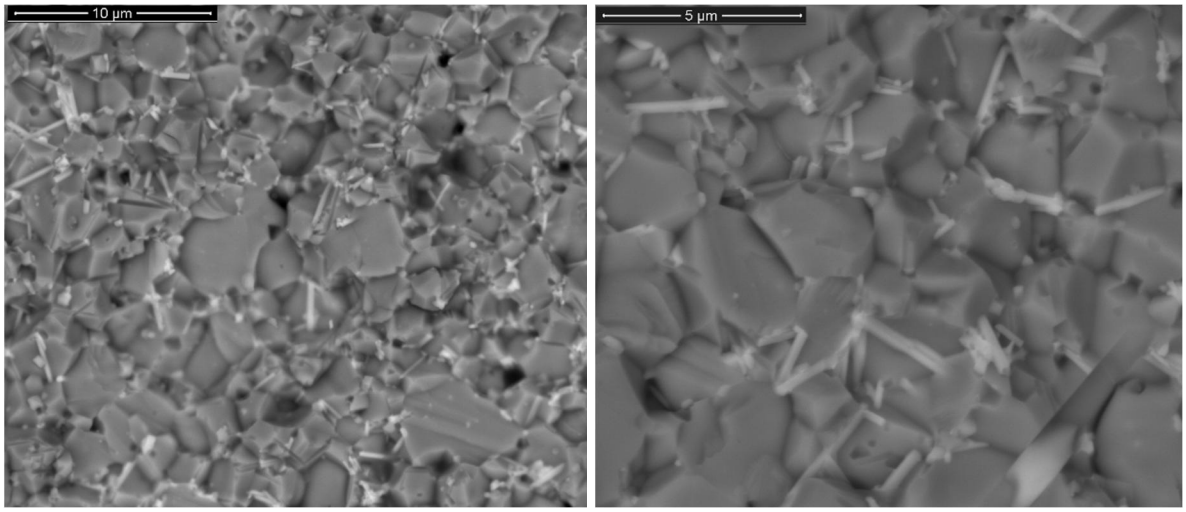
Fig. 5a presents a schematic view of the cross-section of a multilayer varistor. Fig. 5b illustrates a multilayer varistor after lamination and sintering processes. The thicknesses of ceramic layers between internal electrodes after sintering were about 105 μm for 10-layer varistors and about 160 μm for 5-layer varistors.



(a) (b)

Fig. 5. (a) Schematic view of a multilayer varistor, (b) multilayer varistor after lamination and sintering processes

In Fig. 6 and Fig. 7, BSE *(Back Scattered Electrons)* images of cross-sections of a fired multilayer varistor are presented. The microstructure of the varistor layers is fine-grained and well densified. As can be seen from Fig. 6, besides dominating larger ZnO grains (1-5 μm in diameter), there are smaller and brighter grains, and needle-like crystallites containing elements with higher atomic number. Fig. 7 illustrates a good cooperation with the platinum electrodes. No cracks or delaminations resulting from the thermal treatment were observed at the electrode-ceramic layer boundaries.



(a) (b)

Fig. 6. Back-scattered electron images of a fractured cross-section of the varistor ceramic layer

Fig. 8 displays the results of the chemical microanalysis using EDS method for points 1-4 marked in Fig. 7. Point 1 corresponds to the interior of a large ZnO grain. The region around point 2 corresponding to a needle-shaped crystallite contains zinc, praseodymium, bismuth and silicon. Presumably, it is zinc oxide strongly doped with praseodymium which after sintering at lower temperatures may crystallize in a form of needles, or a separate crystalline phase based on zinc and praseodymium. Further investigations using X-ray diffraction analysis should be carried out to elucidate phase composition of these needle crystallites. The composition determined in the point 3 indicates the presence of zinc, antimony, manganese, cobalt and chromium. It can be ascribed to a grain of the complex spinel phase situated at the grain boundary of the ZnO grains. Point 4 corresponds to Pt electrode.

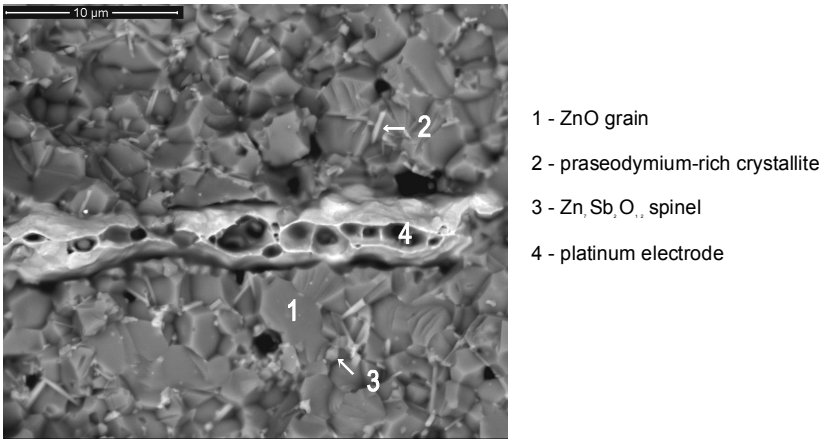
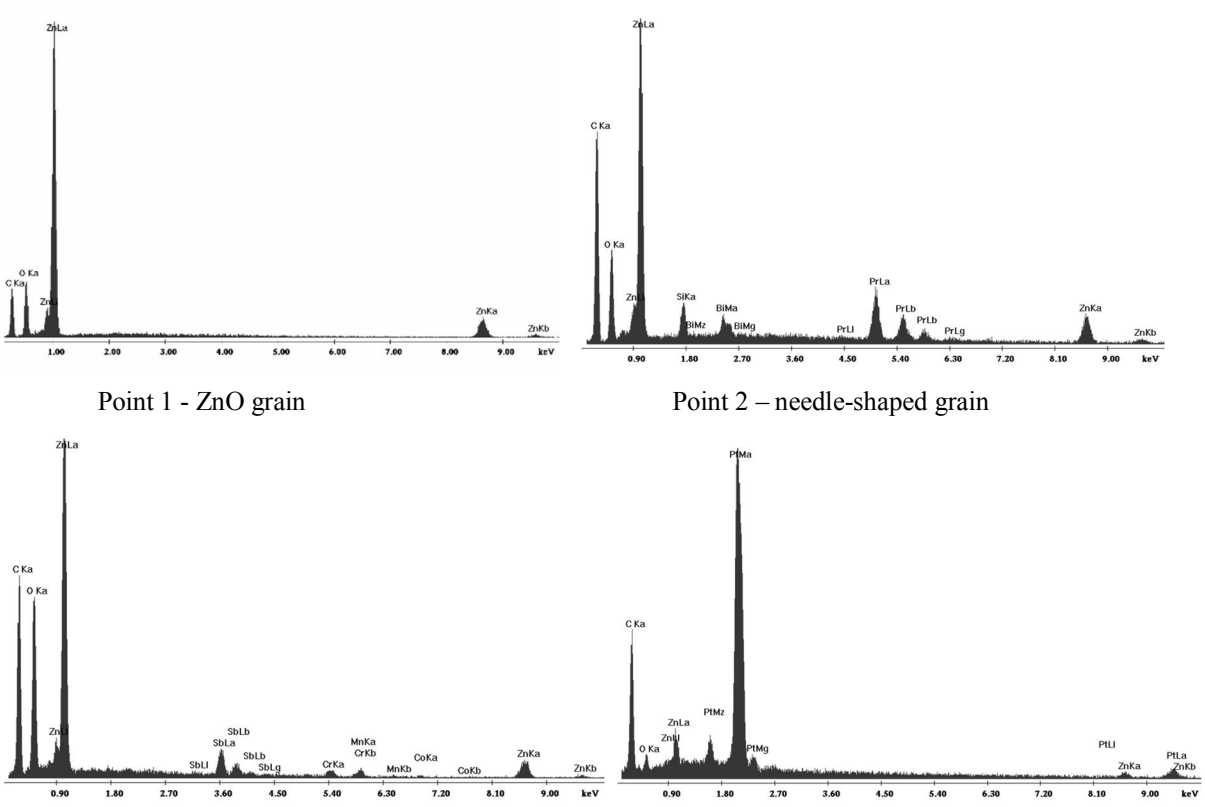


Fig. 7. Back-scattered electron image of a fractured cross-section of a multilayer varistor in the region of the ceramic layer-electrode boundary



Point 1 - ZnO grain

Point 2 – needle-shaped grain

Point 3 – spinel

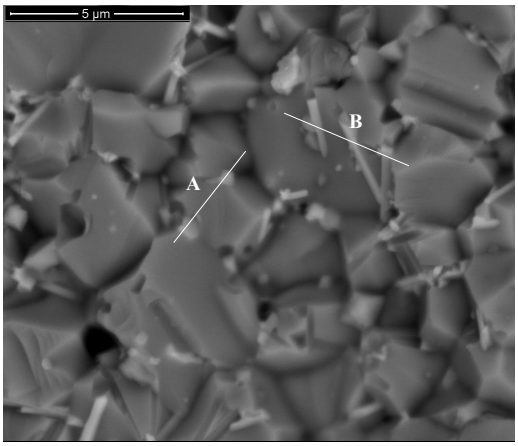
Point 4 – Pt electrode

Fig. 8. The results of the energy-dispersive X-ray microanalysis in the points 1-4 (marked in Fig. 7).

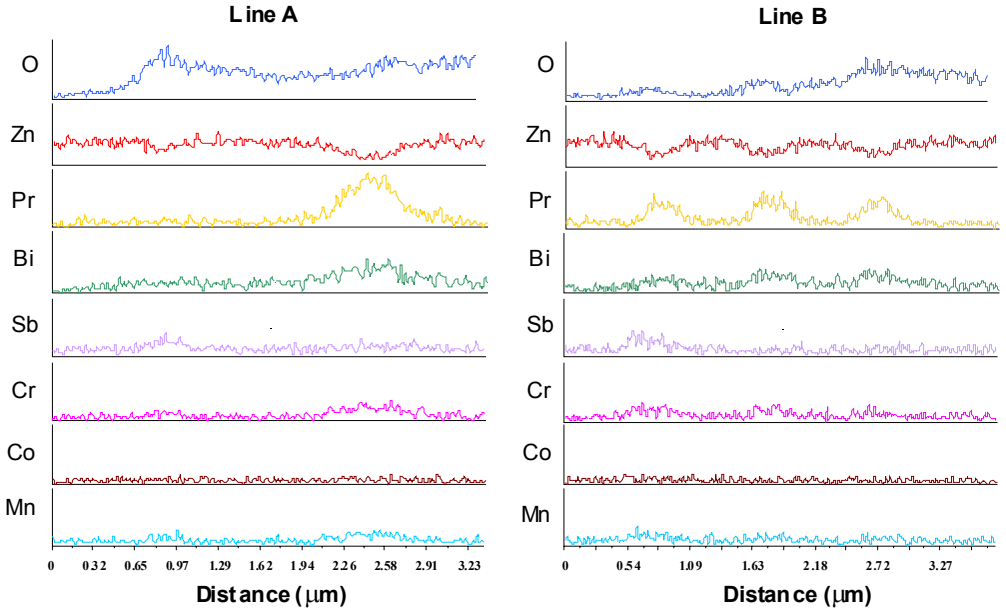
The additional phases represented by points 2 and 3 may contribute to the inhibition of grain growth of ZnO grains and result in formation of fine-grained and uniform microstructure with a small grain size distribution which is desired for multilayer varistors.

In Fig. 9 the microstructure of the varistor layer and the composition along two lines A and B are presented. The line A intersects a large ZnO grain and two smaller grains situated at the boundary of two ZnO grains. It follows from the line analysis that the composition of two smaller grains is not the same. One of these grains contains antimony and is enriched in oxygen and manganese which implies that it may be $Zn_7Sb_2O_{12}$ spinel with a part of ions substituted by Mn. The second small grain at the boundary of ZnO grains contains praseodymium, bismuth, chromium, manganese and exhibits an enhanced oxygen concentration.

The line B intersects a large ZnO grain about 5 μm in diameter, a smaller spherical grain with the diameter less than 0.5 μm and three needle-shaped crystallites. In the region of needles, a significant enrichment in praseodymium, bismuth and chromium is observed. The composition of a spherical grain, presumably being spinel phase, is characterized by an increased level of antimony and manganese.



(a)



(b)

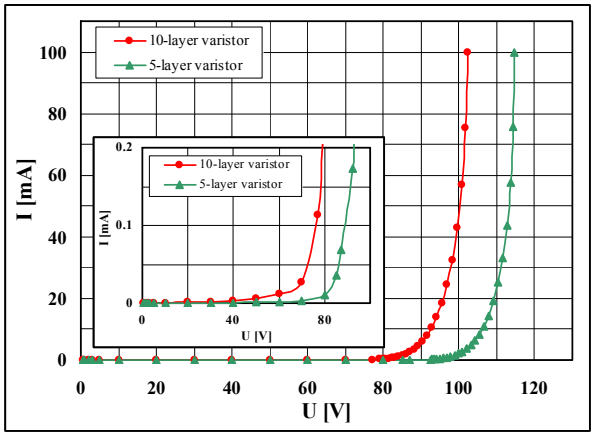
Fig. 9. (a) BSE image of a fractured cross-section of a multilayer varistor, (b) EDS analysis of the content of chemical elements along lines A and B

The SEM observations of varistor layers under a high magnification (80000 x) reveal very thin films (with the thickness of tens of nanometers) surrounding ZnO grains, probably built of glass phase rich in Bi_2O_3.

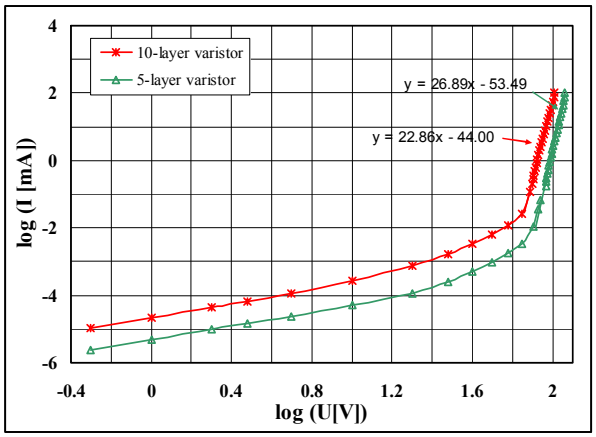
The current-voltage characteristics of the obtained varistors are plotted in different coordinates in Figs. 10a, 10b and 10c. As can be seen from Fig. 10a, for the voltage exceeding 60 V and 80 V for 10-layer and 5-layer varistors, respectively, a rapid increase in current occurs which results from an abrupt decrease in the varistor resistance. Figs. 10b and 10c illustrate a transition from the region of low voltages and currents which is related to a high resistance of the varistor, to the region of

nonlinear characteristic of the varistor which is observed above the breakdown voltage of the potential barrier at grain boundaries. The nonlinearity coefficient determined from the slope of the log I = f (log U) plot is about 23 and 27 for 10-layer and 5-layer varistors, respectively.

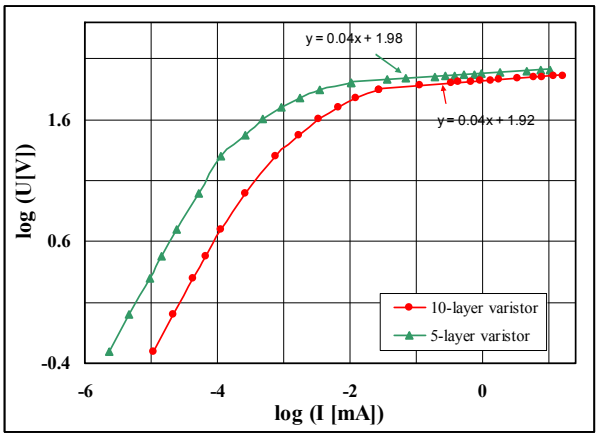
The breakdown voltages and nonlinearity coefficients increase with increasing thickness of the ceramic layer between the internal electrodes of a varistor. This effect is caused by an enhanced number of grain boundaries in his region and is consistent with the results reported by other authors [8].



(a)



(b)



(c)

Fig. 10. Current-voltage characteristic of a multilayer varistor

4. CONCLUSIONS

Tape casting method was used successfully for obtainment of green varistor foils based on ZnO doped with Bi, Sb, Co, Mn, B, Si and Pr oxides. As a result of a sequence of operations including laser cutting, screen printing of platinum electrodes, stacking of green sheets, isostatic lamination and cofiring, multilayer varistors were fabricated. After thermal treatment, ceramic layers were dense and fine-grained and show good cooperation with platinum internal electrodes. SEM and EDS studies reveal the presence of large ZnO grains of 1-5 μm size, submicrometer spinel grains at the boundaries

of ZnO, needle-shaped praseodymium rich crystallites and nanometric Bi_2O_3-rich films surrounding ZnO grains. The breakdown voltage and nonlinearity coefficient are 60 V and 23 for 10-layer varistors, and 80 V and 27 for 5-layer varistors. Both these varistor parameters increase with growing thickness of the ceramic layer between electrodes.

ACKNOWLEDGEMENTS:

The work has been financed by the Polish Ministry of Science and Higher Education under grant N N507 468038.

REFERENCES

1. Levinson, L.M., Philipp, H.R. (1986) Zinc Oxide Varistors - A Review. Ceram. Bull. **65**, pp. 639-646.

2. Clarke, D.R. (1999) Varistor Ceramics. J. Am. Ceram. Soc. **82**, pp. 485-502.

3. Bueno, P.R., Varela, J.A., Longo, E. (2008) SnO_2, ZnO and related polycrystalline compound semiconductors: An overview and review on the voltage-dependent resistance (non-ohmic) feature. J. Eur. Ceram. Soc. **28**, pp. 505-529.

4. Daneu, N., Recnik, A., Bernik, S. (2003) Grain growth control in Sb_2O_3–Doped Zinc Oxide, J. Am. Ceram. Soc. **66**, pp. 1379-1384.

5. Cai, J., Lin, Y.H., Li, M., Nan, C.W. (2007) Sintering temperature dependence of grain boundary resistivity in a rare-earth doped ZnO varistor. J. Am. Ceram. Soc. **90**, pp. 291-294.

6. Alles, A.B., Burdick, V.L. (1991) The effect of liquid-phase sintering on the properties of Pr_6O_{11}-based ZnO varistors. J. Appl. Phys. **70**, pp. 6883-6890.

7. Zhu, J., Qi, G., Yang, H., Wang, F. (2011) Microstructure and electrical properties of Pr_6O_{11} doped ZnO-Bi_2O_3-based varistors. J. Mater.Sci.: Mater. Electron. **22**, pp. 96-100.

8. Kuo, S.T.,Tuan, W.H. (2008) Grain growth behavior of Bi_2O_3-doped ZnO grains in a multilayer varistor. J. Am. Ceram. Soc. **91**, pp. 1572-1579.

9. Kuo, S.T., Tuan, W.H., Lao, Y.W. (2009) Inner Electrodes for Multilayer Varistors. Int. J. Appl. Ceram. Techn. **6**, pp. 223-230.

10. Lee, W.H., Chen, W.T., Lee, Y.C., Lin, S.P., Yang, T. (2006) Relationship between microstructure and electrical properties of ZnO-based multilayer varistor. Jpn. J. Appl. Phys. **45**, pp. 5126-5131.

11. Lee, W.S., Chen, W.T., Lee, Y.C., Yang, T., Su, C.Y., Hu, C.L. (2007) Influence of sintering on microstructure and electrical properties of ZnO-based multilayer varistor (MLV), Ceram. Int. **33**, pp. 1001-1005.

12. Pan, W.H., Kuo, S.T., Tuan, W.H., Chen, H. (2010) Microstructure-Property Relationships for Low-Voltage Varistors , Int. J. Appl. Ceram. Techn. **7**, pp. 1744-7402.

13. Kuo, S.T., Tuan, W.H. (2010) Grain growth behaviour of ZnO-based multilayer varistors. J. Eur. Ceram. Soc, **30**, pp. 525-530.

14. Rubia, M.A., Peiteado, M., Frutos, J., Rubio-Marcos, F., Fernandez, V., Caballero, A.C. (2007) Improved non-linear behaviour of ZnO-based varistor thick films prepared by tape casting and screen printing. J. Eur. Ceram. Soc. **27**, pp. 3887–3891.

15. Peiteado, M., Rubia, M.A., Frutos, J., Jardiel, T. (2009) ZnO-based varistor thick films with high non-linear electrical behavior, J. Electroceram. **23**, pp. 62-66.

16. Wan, S., Lu, W., Wang, X. (2010) Low-Temperature Sintering and Electrical Properties of ZnO-Bi_2O_3-TiO_2-Co_2O_3-$MnCO_3$ Based Varistor with Bi_2O_3-B_2O_3 Frit for Multilayer Chip Varistor Applications. J. Am. Ceram. Soc. **93**, pp. 3319-3323.